Supporting information

Machine Learning Interatomic Potentials Enable First-Principles Multiscale Modeling of Lattice Thermal Conductivity in Graphene/Borophene Heterostructures

Bohayra Mortazavi*[a,b], Evgeny V. Podryabinkin[c], Stephan Roche[d,f],

Timon Rabczuk[g], Xiaoying Zhuang[a,g] and Alexander V. Shapeev[c]

[a]*Chair of Computational Science and Simulation Technology, Department of Mathematics and Physics, Leibniz Universität Hannover, Appelstraße 11,30157 Hannover, Germany.*
[b]*Cluster of Excellence PhoenixD (Photonics, Optics, and Engineering–Innovation Across Disciplines), Gottfried Wilhelm Leibniz Universität Hannover, Hannover, Germany.*
[c]*Skolkovo Institute of Science and Technology, Skolkovo Innovation Center, Nobel St. 3, Moscow 143026, Russia.*
[d]*Catalan Institute of Nanoscience and Nanotechnology (ICN2), CSIC and BIST, Campus UAB, Bellaterra, 08193 Barcelona, Spain.*
[f]*ICREA Institució Catalana de Recerca i Estudis Avancats, 08010 Barcelona, Spain*
[g]*College of Civil Engineering, Department of Geotechnical Engineering, Tongji University, Shanghai, China.*

*bohayra.mortazavi@gmail.com

Related data are availbale via: http://dx.doi.org/10.17632/pbgscy3ptg.1

Content:

1. Training a moment tensor potential (MTP).

1.1 Access to the MLIP package.

MLIP is a software package implementing MTP. It is distributed upon sending a reasonable request to Alexander Shapeev at *a.shapeev@skoltech.ru*. Please note that for the classical molecular dynamics simulations using the MTPs, the related plugin with LAMMPS [1] has to be also installed.

1.2 Creating training sets.

As explained in the original manuscript, the training sets are created by conducting the ab-initio molecular dynamics (AIMD) simulations at different temperatures. In our work, we employed the *Vienna Ab-initio Simulation Package* (VASP)[2–4] with generalized gradient approximation (GGA) and Perdew–Burke–Ernzerhof (PBE)[5]. In the Mendeley dataset, the folder entitled "*AIMD-inputs*", two samples of VASP input files (namely, POSCAR, POTCAR, INCAR and KPOINTS) for pristine borophene and a graphene/borophene heterostructure at 300 K are included. After the completion of AIMD simulations, OUTCAR file can be used to create the training set (*train.cfg*) with the following command:

./mlp convert-cfg OUTCAR train.cfg --input-format=vasp-outcar

Using the aforementioned command all the configurations will be included in the training set. Shortening of the training set (creating subsamples) can be achieved using the following command:

./mlp subsample train.cfg subsample.cfg 10

In the mentioned case, each first of every 10 snapshots in the original "*train.cfg*" will be written to the *"subsample.cfg".* The subsampled training sets at different temperatures or structures should be then merged together to create the final training set, which can be achieved using the Linux *"Cat Command"*.

1.3 Training of MTPs.

Training of MTP can be achieved by solving the following minimization problem:

$$\sum_{k=1}^{K}\left[w_e\left(E_k^{\mathrm{AIMD}}-E_k^{\mathrm{MTP}}\right)^2+w_f\sum_{i}^{N}\left|f_{k,i}^{\mathrm{AIMD}}-f_{k,i}^{\mathrm{MTP}}\right|^2+w_s\sum_{i,j=1}^{3}\left|\sigma_{k,ij}^{\mathrm{AIMD}}-\sigma_{k,ij}^{\mathrm{MTP}}\right|^2\right]\rightarrow \min,$$

where E_k^{AIMD}, $f_{k,i}^{\mathrm{AIMD}}$ and $\sigma_{k,ij}^{\mathrm{AIMD}}$ are the energy, atomic forces and stresses in the training set, respectively, and E_k^{MTP}, $f_{k,i}^{\mathrm{MTP}}$ and $\sigma_{k,ij}^{\mathrm{MTP}}$ are the corresponding values calculated with the MTP, *K* is the number of the configurations in the training set, *N* is the number of atoms in every and w_e, w_f and w_s are the non-negative weights that express the importance of energies and forces and stresses in the optimization problem, respectively, which in our study were set to 1, 0.1 and

0.001, respectively. We note that the weights for the energy and force are the default values. As an example, the training of a MTP can be achieved using the following command:

mpirun -n n_cores ./mlp train p.mtp train.cfg --energy-weight=1 --force-weight=0.1 --stress-weight=0.001 --max-iter=2000 --curr-pot-name=p.mtp --trained-pot-name=p.mtp

In the mentioned case, where "*n_cores*" is the number of cores used for parallel training of MTP, *"p.mtp"* is the input/output (curr-pot-name/trained-pot-name) MTP file, "*train.cfg*" is the training set in internal *.cfg MLIP format, the option "*max-iter*" determines the maximum number of iterations in the optimization algorithm. The options "*energy-weight*", "*force-weight*", and "*stress-weight*", respectively, define the w_e, w_f and w_s weights explained earlier.

Important note:

As discussed in the preparation of training sets, from the complete sets of AIMD configurations, only subsamples are selected for the training of first MTPs. Nonetheless, some critical configurations that could result in the improved stability of trained MTPs may have been missed in the created subsamples. Therefore, the accuracy of the developed MTP "*p.mtp*" using the initial subsampled training set "*train.cfg*" should be once again checked over the full AIMD configurations "*trainF.cfg"*, and the configurations with high extrapolations grades [6] should be selected, and written to the file "*trainN.cfg", via the following command:*

./mlp select-add p.mtp train.cfg trainF.cfg trainN.cfg

The selected configurations "*trainN.cfg"* should be added to the original training sets "*train.cfg*" and the final MTP will be developed by retraining of new clean potentials over the updated training set. This way, the efficient use of conducted AIMD simulations will be guaranteed.

1.4 Structure of MTPs.

MTP belongs to the family of machine-learning interatomic potentials by which potentials show flexible functional form that allows for systematically increasing of the accuracy with an increase in the number of parameters and the size of the training. In the folder entitled "Untrained-MTPs", we included three samples of clean MTPs. Depending on the number of parameters, the appropriate MTP should be chosen. Prior to training there are few parameters to be adjusted, such as the "*species_count*", "*min_dist*" and "*max_dist*" which, respectively, define the number of element in the system, minimum atomic distance and cutoff distance of the potential. Please note that "*species_count*"and "*min_dist*" will be updated after the training process. Like the classical potentials, by increasing the cutoff distance more neighbors will be included in the calculations which will increase the computational costs accordingly. The number of parameters in a MTP can be calculated via:

$$\textbf{\textit{species\_count}}^2\textbf{\textit{.radial\_basis\_size.radial\_funcs\_count+alpha\_scalar\_moments+1}}$$

Please note that *"radial_funcs_count*" and "*alpha_scalar_moments*" are the fixed features of a particular MTP and only "*radial_basis_size*" can be manually changed to adjust the number of constants.

1.5 Evaluation of phononic properties using the MTPs.

In our previous work, we included the full details and numerous examples for the evaluation of phononic properties using the MTP and PHONOPY [7] package in a public Mendeley dataset, please refer to: http://dx.doi.org/10.17632/7ppcf7cs27.1

2. Graphene/borophene grain boundaries.

Because of the different atomic structures of borophene and graphene and depending on the various tilting angles of intersecting crystals, graphene/borophene grain boundaries can show diverse configurations. In this work, as shown in Fig. 2a we constructed 10 different grain boundaries. Since plane-wave AIMD calculations were conducted, in order to create the training sets, the constructed models are ought to be periodic in planar directions. This way, in every graphene/borophene heterostructure model, two different grain boundaries were formed. In this work, we have chosen 6 graphene and borophene heterostructure models, and from those we have chosen 10 different grain boundaries for classical NEMD simulations. In the following illustration, these 6 models are illustrated. Constructed graphene/borophene heterostructure in the VASP native POSCAR format are included in the "*Graphene-Borophene-Heterostructures*" folder of the dataset:

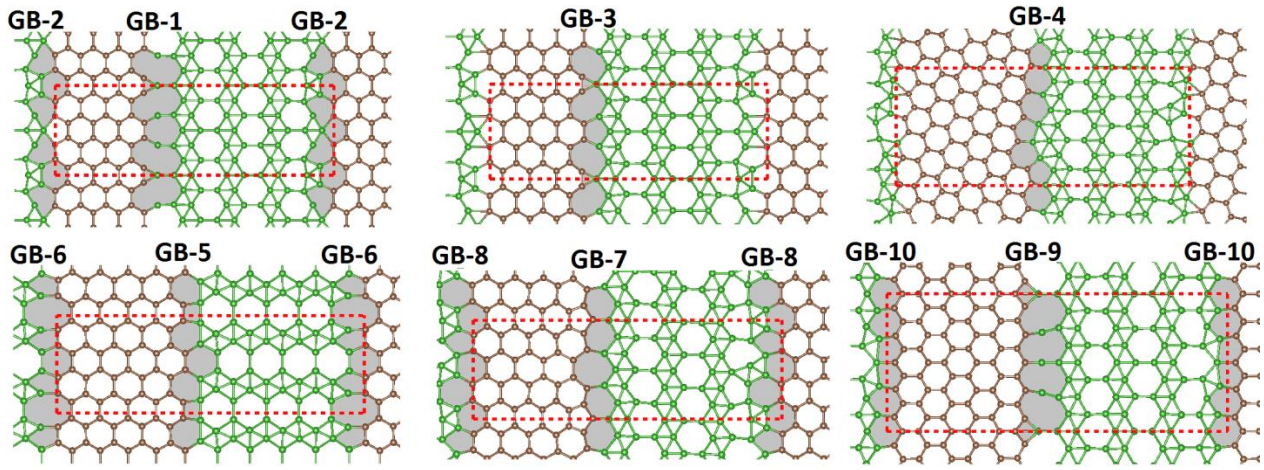

Fig. S1, Constructed graphene/borophene heterostructures for creating the training data. The dashed red-lines exhibit the boundary of models.

We examined the accuracy of trained MTPs for the constructed graphene/borophene heterostructures by conducting the AIMD simulations at 300 K for additional 4000 time steps. By including the original 1000 AIMD trajectories at 300 K, the final trajectories for every model include 5000 configurations. In the following table, the errors of the originally trained MTPs over 5000 AIMD configurations are summarized. Notably, as it can be seen from the results shown Table S1, the average absolute errors in different models are in less than 4 meV, which confirms the high accuracy of developed MTPs.

Table S1, Calculated errors of developed MTPs for 5000 AIMD configurations at 300 K.

	Graphene/borophene heterostructures models					
	GB1 & GB2	GB3	GB4	GB5 & GB6	GB7 & GB8	GB9 & GB10
C and B atoms, respectively	32 and 48	32 and 45	56 and 61	40 and 40	37 and 45	60 and 64
Average absolute difference in energy/atom (meV)	3.4	2.2	1.4	1.5	2.0	1.0
RMS of absolute difference in energy/atom (meV)	4.0	2.6	1.8	1.9	2.7	1.3

3. NEMD simulation using the MTP.

In the provided Mendeley dataset, we included a sample of developed NEMD models for the calculation of a graphene/borophene grain boundary thermal conductance (find "*NEMD-Example*" folder). In order to define the interatomic potential type, in the LAMMPS (*"in.thermal"* in our example) script one has to use the following commands:

pair_style mlip mlip.ini
***pair_coeff * ***

in this case, "*mlip.ini*" is the interface with MLIP package, which includes the path to the trained MTP potential file (find "*mlip:load-from p.mtp*"). The type of atoms in a MTP starts from 0 whereas in LAMMPS starts from 1, such that atomic type of 1 in the MTP (or in the training set) matches to the atomic type of 2 in the LAMMPS script. In the NEMD calculations, after applying the temperature difference at two ends and complete equilibration of the system, the applied heat fluxes by the NVT method to the hot and cold reservoirs and established temperature gradient will be averaged and recorded, to calculate the thermal conductivity or thermal conductance at the interface. In the provided example, heat fluxes and averaged temperatures at every slab are written in the *"fnvt.txt"* and "*T-X.txt*", respectively.

4. Phonon dispersion of graphene and borophene

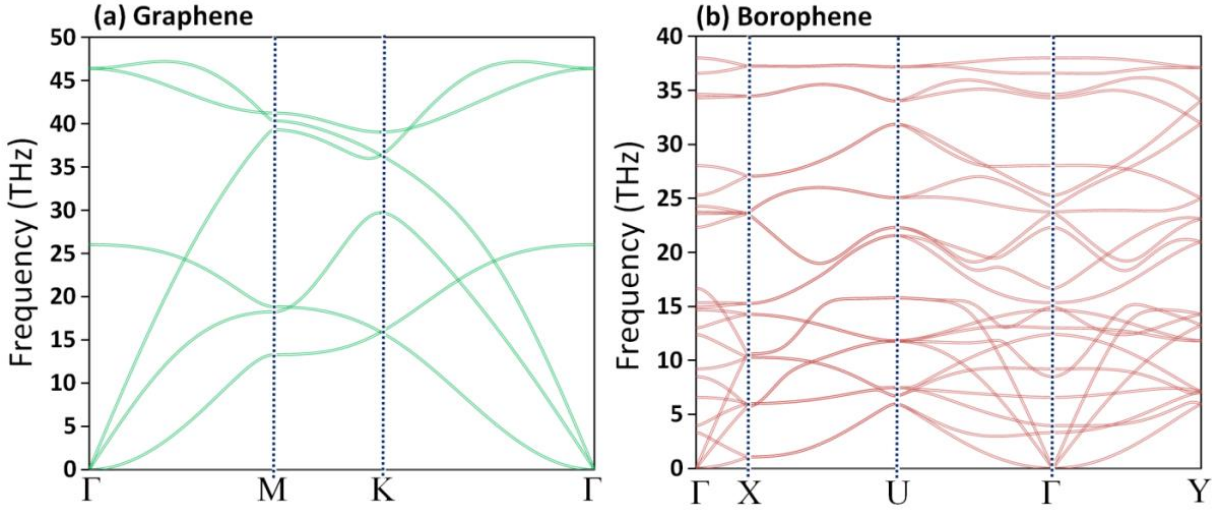

Fig. S2, Phonon dispersion relations of (a) graphene and (b) borophene. In this case the rectangular unit cell was considered for borophene.

5. MTP/ShengBTE interface.

ShengBTE [8] is a package for computing the lattice thermal conductivity on the basis of a full iterative solution to the Boltzmann transport equation. Its main inputs are sets of second- and third-order interatomic force constants and a CONTROL file for the adjustment of computational details. In this work, the calculation of anharmonic interatomic force constants is substantially accelerated by substituting DFT simulations with the MTP-based solution. For the calculation of anharmonic interatomic force constants, ShengBTE [8] provides a script, *"thirdorder.py"*, implementing a real-space supercell approach to anharmonic IFC calculations. In this approach, according to the defined supercell size and cutoff distance, the input geometries for the force constant calculations will be generated. For compatibility with *"cfg"*-file format, the *"thirdorder_vasp.py"* script is modified. Moreover, we developed an additional script *"fake_vasp_calcs.py*", which uses the MTP-based calculated forces and artificially create the VASP output files of "vasprun.xml". This approach provides the possibility of direct comparison of forces by MTP and VASP.

In the folder "*MTP-ShengBTE-Examples*" the complete input files for the graphene, silicon and InAs are included. For every structure, the subfolder entitled "*ShengBTE-inputs*" includes the complete input files for the ShengBTE solution (namely: CONTROL, FORCE_CONSTANTS_2ND and FORCE_CONSTANTS_3RD). Using the data provided in the subfolder called "*Anharmonic-MTP*", a user will be able to reproduce the anharmonic interatomic force constants using the previously trained MTP instead of DFT simulations. To this aim, for every structure we included a shell script for complete calculations, named "*getFC.sh*". Please note that "*p.mtp*", "*mlip.ini*" and relate python scripts should be all in this folder for complete calculations.

6. MTP/BTE results for graphene.

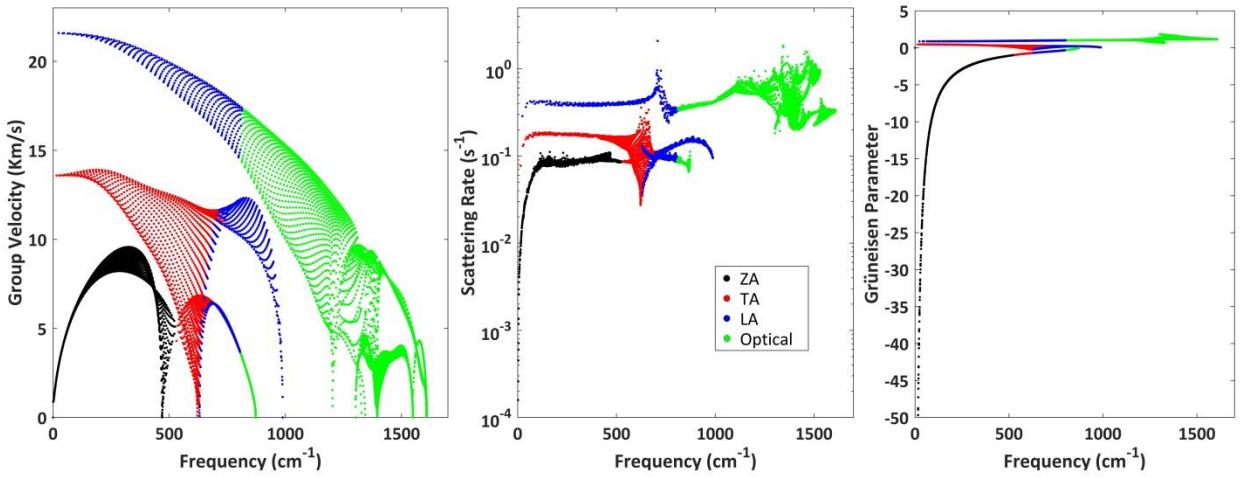

Fig. S3, Contribution of ZA, TA, LA and optical modes on the phonon group velocity, scattering rate and Grüneisen parameter of single-layer graphene as a function of frequency acquired on the basis of MTP/BTE solution.

Table S2, Comparison of thermal conductivity of single-layer graphene predicted using the MTP/BTE with different experimental and full-DFT/BTE theoretical reports.

Thermal conductivity (W/mK)	Method
3600 [300 K]	Present study, MTP/BTE
~3080–5300 [300 K]	Raman spectroscopy [9,10]
4127±539 [300 K]	Raman spectroscopy [11]
1500-5000 [300 K]	Raman spectroscopy [12]
2500±(+1100, -1050) [300 K]	Raman spectroscopy [13]
2500 [300 K]	Micro electro-thermal (micro-resistance thermometer) [14]
1689-1813 ±100 [300 K]	Micro electro-thermal (micro-resistance thermometer) [15]
2430±190 [335 K]	Scanning thermal microscopy [16]
632 [300 K]	Raman spectroscopy [17]
∼1800 [325 K]	Raman spectroscopy [18]
2500 [310 K]	Raman spectroscopy [19]
3100±1000 [350 K]	Raman spectroscopy [20]
1937–2298 [300 K]	Micro electro-thermal (micro-resistance thermometer) [21]
3720 [300 K]	DFT [PBE]/BTE [22]
3550 [300 K]	DFT [PBE]/BTE [23]
3000 [300 K]	DFT [PBE]/BTE [24]
3600 [300 K]	DFT/BTE [25]
3590 [300 K]	DFT [PBE]/BTE [26]
3150 [300 K]	DFT [PBE]/BTE [27]
1936 [300 K]	DFT [PBE]/BTE [28]
5500 [300 K]	DFT [PBE]/BTE [29]
3095 [300 K]	DFT [PBE]/BTE [30]
3845 [300K]	DFT [PBE]/BTE [31]
3288 [300 K]	DFT [PBE]/BTE [32]

7. MTP/BTE results for bulk silicon and InAs.

To further examine the accuracy of proposed MTP/BTE approach in conjunction with the ShengBTE [8] software, we also study the thermal conductivity of bulk silicon and InAs, the examples considered in the original manuscript for ShengBTE [8]. We used VASP [2–4] package and PBE/GGA method with plane-wave cutoff energies of 330 and 300 eV for the silicon and InAs, respectively. The lattice constant of silicon and InAs were found to be 5.47 and 6.06 Å, respectively, which match closely with the those reported in Ref. [8]. The second-order force constants are obtained by DFPT simulations over 5×5×5 supercells using a 2×2×2 Monkhorst-Pack [33] k-point grid along with the PHONOPY code [7]. For the consistency with Ref. [8], anharmonic force constants are acquired by considering the interactions with the fourth nearest neighbours. Training sets are acquired by conducting the AIMD simulations at temperatures of 100, 300, 500 and 800 K for 1000 time steps. MTPs with 901 and 1009 parameters are trained for silicon and InAs, respectively. For the anharmonic force constants calculations, we also used 5×5×5 supercells. For the case of InAs, dielectric tensor and Born effective charges are also included in the calculations and the values were taken from the ShengBTE [8] examples. Fig. S4 compares the results by the MTP/BTE method with experimental and full-DFT/BTE solutions for

the thermal conductivity of silicon and InAs. As it is clear, MTP/BTE results match closely with experimental and previous theoretical studies.

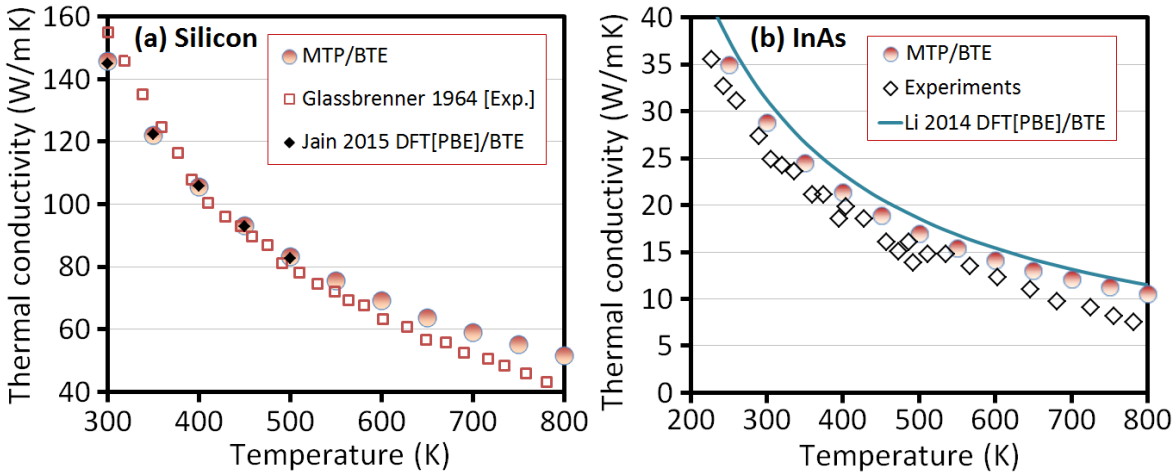

Fig. S4, Thermal conductivity of (a) silicon and (b) InAs predicted by the MTP/BTE and previous theoretical studies by Jain et al. [34] and Li et al. [8]. The experimental results for silicon and InAs were taken from [35] and [36,37],respectively.

References

[1] S. Plimpton, Fast Parallel Algorithms for Short-Range Molecular Dynamics, J. Comput. Phys. 117 (1995) 1–19. doi:10.1006/jcph.1995.1039.

[2] G. Kresse, J. Furthmüller, Efficiency of ab-initio total energy calculations for metals and semiconductors using a plane-wave basis set, Comput. Mater. Sci. 6 (1996) 15–50. doi:10.1016/0927-0256(96)00008-0.

[3] G. Kresse, J. Furthmüller, Efficient iterative schemes for ab initio total-energy calculations using a plane-wave basis set, Phys. Rev. B. 54 (1996) 11169–11186. doi:10.1103/PhysRevB.54.11169.

[4] G. Kresse, From ultrasoft pseudopotentials to the projector augmented-wave method, Phys. Rev. B. 59 (1999) 1758–1775. doi:10.1103/PhysRevB.59.1758.

[5] J. Perdew, K. Burke, M. Ernzerhof, Generalized Gradient Approximation Made Simple., Phys. Rev. Lett. 77 (1996) 3865–3868. doi:10.1103/PhysRevLett.77.3865.

[6] E. V Podryabinkin, A. V Shapeev, Active learning of linearly parametrized interatomic potentials, Comput. Mater. Sci. 140 (2017) 171–180. doi:10.1016/j.commatsci.2017.08.031.

[7] A. Togo, I. Tanaka, First principles phonon calculations in materials science, Scr. Mater. 108 (2015) 1–5. doi:10.1016/j.scriptamat.2015.07.021.

[8] W. Li, J. Carrete, N.A. Katcho, N. Mingo, ShengBTE: A solver of the Boltzmann transport equation for phonons, Comput. Phys. Commun. 185 (2014) 1747–1758. doi:10.1016/j.cpc.2014.02.015.

[9] S. Ghosh, I. Calizo, D. Teweldebrhan, E.P. Pokatilov, D.L. Nika, A.A. Balandin, W. Bao, F. Miao, C.N. Lau, Extremely high thermal conductivity of graphene: Prospects for thermal management applications in nanoelectronic circuits, Appl. Phys. Lett. 92 (2008) 1–4.

doi:10.1063/1.2907977.
[10] A.A. Balandin, S. Ghosh, W. Bao, I. Calizo, D. Teweldebrhan, F. Miao, C.N. Lau, Superior thermal conductivity of single-layer graphene, Nano Lett. 8 (2008) 902–907. doi:10.1021/nl0731872.
[11] S. Ghosh, W. Bao, D.L. Nika, S. Subrina, E.P. Pokatilov, C.N. Lau, A.A. Balandin, Dimensional crossover of thermal transport in few-layer graphene, Nat. Mater. 9 (2010) 555–558. doi:10.1038/nmat2753.
[12] L.A. Jauregui, Y. Yue, A.N. Sidorov, J. Hu, Q. Yu, G. Lopez, R. Jalilian, D.K. Benjamin, D.A. Delkd, W. Wu, Z. Liu, X. Wang, Z. Jiang, X. Ruan, J. Bao, S.S. Pei, Y.P. Chen, Thermal Transport in Graphene Nanostructures: Experiments and Simulations, in: 2010: pp. 73–83. doi:10.1149/1.3367938.
[13] W. Cai, A.L. Moore, Y. Zhu, X. Li, S. Chen, L. Shi, R.S. Ruoff, Thermal transport in suspended and supported monolayer graphene grown by chemical vapor deposition, Nano Lett. 10 (2010) 1645–1651. doi:10.1021/nl9041966.
[14] V.E. Dorgan, A. Behnam, H.J. Conley, K.I. Bolotin, E. Pop, High-Field Electrical and Thermal Transport in Suspended Graphene, Nano Lett. 13 (2013) 4581–4586. doi:10.1021/nl400197w.
[15] X. Xu, L.F.C. Pereira, Y. Wang, J. Wu, K. Zhang, X. Zhao, S. Bae, C. Tinh Bui, R. Xie, J.T.L. Thong, B.H. Hong, K.P. Loh, D. Donadio, B. Li, B. Özyilmaz, Length-dependent thermal conductivity in suspended single-layer graphene, Nat. Commun. 5 (2014) 1–6. doi:10.1038/ncomms4689.
[16] K. Yoon, G. Hwang, J. Chung, H.G. Kim, O. Kwon, K.D. Kihm, J.S. Lee, Measuring the thermal conductivity of residue-free suspended graphene bridge using null point scanning thermal microscopy, Carbon N. Y. 76 (2014) 77–83. doi:10.1016/j.carbon.2014.04.051.
[17] C. Faugeras, B. Faugeras, M. Orlita, M. Potemski, R.R. Nair, A.K. Geim, Thermal conductivity of graphene in corbino membrane geometry, ACS Nano. (2010). doi:10.1021/nn9016229.
[18] J.U. Lee, D. Yoon, H. Kim, S.W. Lee, H. Cheong, Thermal conductivity of suspended pristine graphene measured by Raman spectroscopy, Phys. Rev. B - Condens. Matter Mater. Phys. 83 (2011) 1–4. doi:10.1103/PhysRevB.83.081419.
[19] S. Chen, Q. Li, Q. Zhang, Y. Qu, H. Ji, R.S. Ruoff, W. Cai, Thermal conductivity measurements of suspended graphene with and without wrinkles by micro-Raman mapping, Nanotechnology. 23 (2012). doi:10.1088/0957-4484/23/36/365701.
[20] S. Chen, A.L. Moore, W. Cai, J.W. Suk, J. An, C. Mishra, C. Amos, C.W. Magnuson, J. Kang, L. Shi, R.S. Ruoff, Raman Measurements of Thermal Transport in Suspended Monolayer Graphene of Variable Sizes in Vacuum and Gaseous Environments, ACS Nano. 5 (2011) 321–328. doi:10.1021/nn102915x.
[21] H. Wang, K. Kurata, T. Fukunaga, X. Zhang, H. Takamatsu, Width dependent intrinsic thermal conductivity of suspended monolayer graphene, Int. J. Heat Mass Transf. 105 (2017) 76–80. doi:10.1016/j.ijheatmasstransfer.2016.09.054.
[22] B. Peng, H. Zhang, H. Shao, Y. Xu, G. Ni, R. Zhang, H. Zhu, Phonon transport properties of two-dimensional group-IV materials from ab initio calculations, Phys. Rev. B. (2016). doi:10.1103/PhysRevB.94.245420.
[23] Y. Gao, H. Wang, M. Sun, Y. Ding, L. Zhang, Q. Li, First-principles study of intrinsic phononic

thermal transport in monolayer C3N, Phys. E Low-Dimensional Syst. Nanostructures. 99 (2018) 194–201. doi:10.1016/j.physe.2018.02.012.
[24] S. Kumar, S. Sharma, V. Babar, U. Schwingenschlögl, Ultralow lattice thermal conductivity in monolayer C 3 N as compared to graphene, J. Mater. Chem. A. 5 (2017) 20407–20411. doi:10.1039/C7TA05872A.
[25] G. Fugallo, A. Cepellotti, L. Paulatto, M. Lazzeri, N. Marzari, F. Mauri, Thermal Conductivity of Graphene and Graphite: Collective Excitations and Mean Free Paths, Nano Lett. 14 (2014) 6109–6114. doi:10.1021/nl502059f.
[26] X. Wu, V. Varshney, J. Lee, T. Zhang, J.L. Wohlwend, A.K. Roy, T. Luo, Hydrogenation of Penta-Graphene Leads to Unexpected Large Improvement in Thermal Conductivity, Nano Lett. 16 (2016) 3925–3935. doi:10.1021/acs.nanolett.6b01536.
[27] Y. Dong, C. Zhang, M. Meng, M.M. Groves, J. Lin, Novel two-dimensional diamond like carbon nitrides with extraordinary elasticity and thermal conductivity, Carbon N. Y. 138 (2018) 319–324. doi:10.1016/j.carbon.2018.06.016.
[28] G. Qin, Z. Qin, H. Wang, M. Hu, On the diversity in the thermal transport properties of graphene: A first-principles-benchmark study testing different exchange-correlation functionals, Comput. Mater. Sci. 151 (2018) 153–159. doi:10.1016/j.commatsci.2018.05.007.
[29] A. Taheri, C. Da Silva, C.H. Amon, First-principles phonon thermal transport in graphene: Effects of exchange-correlation and type of pseudopotential, J. Appl. Phys. 123 (2018) 215105. doi:10.1063/1.5027619.
[30] H. Wang, G. Qin, Z. Qin, G. Li, Q. Wang, M. Hu, Lone-Pair Electrons Do Not Necessarily Lead to Low Lattice Thermal Conductivity: An Exception of Two-Dimensional Penta-CN2, J. Phys. Chem. Lett. 9 (2018) 2474–2483. doi:10.1021/acs.jpclett.8b00820.
[31] X. Tan, H. Shao, T. Hu, G. Liu, J. Jiang, H. Jiang, High thermoelectric performance in two-dimensional graphyne sheets predicted by first-principles calculations, Phys. Chem. Chem. Phys. 17 (2015) 22872–22881. doi:10.1039/c5cp03466c.
[32] L. Lindsay, W. Li, J. Carrete, N. Mingo, D.A. Broido, T.L. Reinecke, Phonon thermal transport in strained and unstrained graphene from first principles, Phys. Rev. B. 89 (2014) 155426. doi:10.1103/PhysRevB.89.155426.
[33] H. Monkhorst, J. Pack, Special points for Brillouin zone integrations, Phys. Rev. B. 13 (1976) 5188–5192. doi:10.1103/PhysRevB.13.5188.
[34] A. Jain, A.J.H. McGaughey, Effect of exchange–correlation on first-principles-driven lattice thermal conductivity predictions of crystalline silicon, Comput. Mater. Sci. 110 (2015) 115–120. doi:https://doi.org/10.1016/j.commatsci.2015.08.014.
[35] C.J. Glassbrenner, G.A. Slack, Thermal Conductivity of Silicon and Germanium from 3\ifmmode^\circ\else\textdegree\fi{}K to the Melting Point, Phys. Rev. 134 (1964) A1058–A1069. doi:10.1103/PhysRev.134.A1058.
[36] R. Bowers, R.W. Ure, J.E. Bauerle, A.J. Cornish, InAs and InSb as Thermoelectric Materials, J. Appl. Phys. 30 (1959) 930–934. doi:10.1063/1.1735264.
[37] G. Le Guillou, H.J. Albany, Phonon Conductivity of InAs, Phys. Rev. B. 5 (1972) 2301–2308. doi:10.1103/PhysRevB.5.2301.